J|A|C|S
ARTICLES

Published on Web 04/26/2010

Self-Assembly of Flexible One-Dimensional Coordination Polymers on Metal Surfaces

Daniel Heim,[†] David Écija,*[,†] Knud Seufert,[†] Willi Auwärter,*[,†] Claudia Aurisicchio,[§] Chiara Fabbro,[#] Davide Bonifazi,*[,§,#] and Johannes V. Barth[†]

Physik Department E20, Technische Universität München, D-85748 Garching, Germany, Department of Chemistry, University of Namur, Rue de Bruxelles 61, B-5000, Namur, Belgium, and Department of Pharmaceutical Sciences, University of Trieste, Piazzale Europa 1, I-34127 Trieste, Italy

Received February 5, 2010; E-mail: david.ecija.fernandez@ph.tum.de; wilhelm.auwaerter@ph.tum.de; davide.bonifazi@fundp.ac.be

Abstract: We employed a *de novo* synthesized porphyrin module to construct one-dimensional (1D) Cu-coordinated polymers on Cu(111) and Ag(111) surfaces. The programmed geometry and functionality of the molecular module together with its conformational flexibility and substrate interaction yields sinuous metal−organic polymeric assemblies, based on an unusual two-fold Cu−pyridyl coordination motif. An analysis of scanning tunneling microscopy (STM) data reveals the occurrence of two enantiomers, resulting from the surface confinement that deconvolutes the module in 2D-chiral conformational isomers. The stereoisomers exhibit site-specific surface anchoring, from whence three discrete orientations are possible for each species. Their sequence and mutual arrangement determine direction and curvature of the metal−organic chains. The Cu-coordinated polymers are very similar on both Cu(111) and Ag(111), where their formation is induced by intrinsic and coevaporated adatoms, respectively, which indicates that the lateral bonding motif is predominantly independent of the substrate. In addition, molecular manipulation experiments show the collective motion of entire segments of the Cu-coordinated multi-porphyrin polymers.

Introduction

The engineering of supramolecular coordination polymers and networks developed into a major field of research over the last decades.[1−3] The extensive studies are motivated by both the challenge to design architectures with increasing finesse and the large application potential provided. Herein the understanding and control of supramolecular isomerism, i.e., the existence of diverse network superstructures achieved with the same molecular building blocks,[2] has been recognized as a crucial issue for the development of third-generation functional networks.[3,4] Notably, the use of flexible ligands, which may undergo conformational changes and adapt to their local environment, can be used to achieve isomeric network architectures.

Recently, well-defined metal surfaces have been employed as platforms to build new kinds of coordination polymers and nanostructures.[5] By a careful selection of the linkers (most frequently organic backbones with pyridyl, carbonitrile, or carboxylate functional groups), the metal center (Cu, Fe, Co, and Au), the substrate, and the environmental condition (mostly solid−liquid interfaces or under ultrahigh vacuum (UHV)), an impressive number of low-dimensional coordination polymers or networks (extending in one dimension (1D)[6−8] or 2D[9−12]) have been obtained. These coordination architectures quite generally comprise unusual coordination motifs, not encountered

[†] Technische Universität München.
[§] University of Namur.
[#] University of Trieste.

(1) Blake, A. J.; Champness, N. R.; Hubberstey, P.; Li, W.-S.; Withersby, M. A.; Schröder, M. *Coord. Chem. Rev.* **1999**, *183*, 117. Kitagawa, S.; Kitaura, R.; Noro, S. *Angew. Chem., Int. Ed.* **2004**, *43*, 2334–2375.
(2) Moulton, B.; Zaworotko, M. *J. Chem. Rev.* **2001**, *101*, 1629–1658.
(3) Robin, A. Y.; Fromm, K. M. *Coord. Chem. Rev.* **2006**, *250*, 2127–2157.
(4) Janiak, C. *Dalton Trans.* **2003**, 2781. Horike, S.; Shimomura, S.; Kitagawa, S. *Nature Chem.* **2009**, *1*, 695–704.
(5) Stepanow, S.; Lin, N.; Barth, J. V. *J. Phys: Condens. Matter* **2008**, *20*, 184002. Lin, N.; Stepanow, S.; Ruben, M.; Barth, J. V. *Top. Curr. Chem.* **2009**, *287*, 1–44. Barth, J. V.; Constantini, G.; Kern, K. *Nature* **2005**, *43*, 671–679.
(6) Semenov, A.; Spatz, J. P.; Möller, M.; Lehn, J.-M.; Sell, B.; Schubert, D.; Weidl, C. H.; Schubert, U. S. *Angew. Chem. Int. Ed* **1999**, *38*, 2547–2550. Dmitriev, A.; Spillmann, H.; Lin, N.; Barth, J. V.; Kern, K. *Angew. Chem., Int. Ed.* **2003**, *41*, 2670–2673. Surin, M.; Samori, P.; Jouaiti, A.; Kyritsakas, N.; Housseini, M. W. *Angew. Chem., Int. Ed.* **2007**, *46*, 245. Marschall, M.; Reichert, J.; Weber-Bargioni, A.; Seufert, K.; Auwärter, W.; Klyatskaya, S.; Zoppellaro, G.; Ruben, M.; Barth, J. V. *Nature Chem.* **2010**, *2*, 131–137.
(7) Classen, T.; Fratesi, G.; Costantini, G.; Fabris, S.; Stadler, F. L.; Kim, C.; de Gironcoli, S.; Baroni, S.; Kern, K. *Angew. Chem., Int. Ed* **2005**, *44*, 6142.
(8) Tait, S. L.; Langner, A.; Lin, N.; Stepanow, S.; Rajadurai, C.; Ruben, M.; Kern, K. *J. Phys. Chem. C* **2007**, *111*, 10982.
(9) Spillmann, H.; Dmitriev, A.; Lin, N.; Messina, P.; Barth, J. V.; Kern, K. *J. Am. Chem. Soc.* **2003**, *125*, 10725–10728. Stepanow, S.; Lingenfelder, M.; Dmitriev, A.; Spillmann, H.; Delvigne, E.; Lin, N.; Deng, X.; Cai, C.; Barth, J. V.; Kern, K. *Nat. Mater.* **2004**, *3*, 229–233. Pawin, G.; Wong, K. L.; Kim, D.; Sun, D.; Bartels, L.; Hong, S.; Rahman, T. S.; Carp, R.; Marsella, M. *Angew. Chem., Int. Ed.* **2008**, *47*, 8442–8445. Kühne, D.; Klappenberger, F.; Decker, R.; Schlickum, U.; Brune, H.; Klyatskaya, S.; Ruben, M.; Barth, J. V. *J. Am. Chem. Soc.* **2009**, *131*, 3881–3883. Shi, Z.; Lin, N. *J. Am. Chem. Soc.* **2009**, *131*, 5376–5377. Lin, N.; Stepanow, S.; Vidal, F.; Barth, J. V.; Kern, K. *Chem. Commun.* **2005**, 1681–1683.

with related compounds in solution or the solid-state. Moreover, they typically present coordinatively unsaturated sites, whereby the metal centers are at the same time in contact with the support, which renders peculiar coordination spheres and metal−ligand bonding arrangements beyond Werner's canonical conception of coordination chemistry.[13] By an appropriate design of the building blocks and a careful choice of the other constituents and assembly pathways, novel physicochemical properties of the resulting systems thus come in reach.[14]

In particular, one of the most appealing systems to study are metal−organic porphyrin-based networks on surfaces, regarding the versatile catalytic and optical properties of the porphyrins.[15] However, up to now only one 2D coordination porphyrins-based network has been published.[16] In this respect, we have recently described the formation of multicomponent cyclic supramolecules, which are formed upon self-assembly of geometrically programmed and conformationally flexible porphyrin modules. In particular, comprehensive scanning tunneling microscopy (STM) investigations showed that discrete and tunable assemblies, such trimeric, tetrameric, pentameric, and hexameric cyclic structures, the area of which could be extended upon combining building blocks with different symmetry, could be obtained.[21] This was the starting point to further investigate the metal-directed assembly in adaptive one-dimensional coordination polymers. We used a complex and flexible porphyrin derivative on Cu(111) and Ag(111) under UHV conditions and copper centers provided either intrinsically by the surface or codeposition. Upon surface confinement the module with two functional pyridyl end groups and *tert*-butyl (*t*-Bu) substituents in trans geometry deconvolutes in conformational isomers because of the distinct surface-induced molecular distortion. Surprisingly, this pathway toward 2D chirality,[17] driven solely by the surface conformational adaptation of achiral, but flexible, molecular species, is rarely addressed in literature.[18,19] We identify a series of isomeric and racemic elementary motifs in the polymeric chains, and show the two-fold pyridyl−Cu−pyridyl coordination bonding between the porphyrin modules. A statistical analysis demonstrates the directionality of the metal−ligand interactions, where a straight isomeric arrangement of the pyridyl−Cu−pyridyl unit prevails.

By means of lateral manipulation with the STM tip, we prove that the metal−organic coordination bonding yields a high flexibility of the polymeric structures on both surfaces. The intermolecular bonding interaction within the polymer is strikingly similar on both Cu(111) and Ag(111), the surfaces of which show a marked variation in chemical reactivity and lattice constants. As a consequence, the porphyrin-based coordination polymers might also be directly formable on insulating layers, thus paving the way for future developments regarding supramolecular nanowires in molecular electronics.[20]

Results and Discussion

Porphyrin derivative **1** is based on a tetrapyrrolic core differently substituted at the four *meso*-positions, presenting two phen-1,4-diyl-ethynyl-pyridyl (PhC≡CPyr) and two 3,5-di-*tert*-butylphenyl (*t*-Bu_2Ph) substituents at the 5,15 and 10,20 *meso*-positions, respectively (cf. Chart 1). The molecule has been synthesized following the experimental protocol recently developed by us.[21]

It has been shown that adsorption on solid surfaces can induce specific porphyrin conformations.[22−24] In particular, for *meso*-phenyl-substituted porphyrins, the dihedral angle between the porphyrin ring and the phenyl groups varies due to a competition between the steric repulsion of the *meso*-substituents with the peripheral hydrogens of the pyrrole units (porphyrin core) and the effect of the π-overlap with the porphyrin ring. The influence of the substrate can modify this angle noticeably due to the π−metal interaction and the atomic corrugation and geometric structure of the surface. In addition, if the dihedral angle falls below 60°, distortions of the porphyrin core occur due to intramolecular steric hindrance,[25] typically changing from planar to saddle-shaped.[23,26] In every case, the final dihedral angle is a compromise between the strength of the molecule−substrate interaction, which would tend to decrease the angle, and the steric hindrance between the *meso*-substituents and the H atoms in the pyrrole groups, which goes in the opposite direction.

The molecular dimensions of **1** were extracted after geometry optimization by the PM3 semi-empirical quantum mechanics method. For the display in Chart 1, a rotation of the *t*-Bu_2Ph moieties was performed to match the aspect of the molecule on the surface (a more precise description follows in the discussion of Figure 3 and in the Supporting Information). Accordingly, in each *meso*-position, one *t*-Bu fragment is brighter than the other (cf. Chart 1b,c). Such differences in apparent height between the two protrusions of a *t*-Bu_2Ph group

(10) Schlickum, U.; Decker, R.; Klappenberger, F.; Zopellaro, G.; Klyatskaya, S.; Ruben, M.; Silanes, I.; Arnau, A.; Kern, K.; Brune, H.; Barth, J. V. *Nano Lett.* **2007**, *7*, 3813–3817.
(11) Stepanow, S.; Lin, N.; Payer, D.; Schlickum, U.; Klappenberger, F.; Zopellaro, G.; Ruben, M.; Brune, H.; Barth, J. V.; Kern, K. *Angew. Chem., Int. Ed.* **2007**, *46*, 710.
(12) Matena, M.; Riehm, T.; Stöhr, M.; Jung, T. A.; Gade, L. H. *Angew. Chem., Int. Ed.* **2008**, *47*, 2414.
(13) Werner, A. Z. *Anorg. Chem.* **1893**, *3*, 267–330; http://www.nobel.se/chemistry/laureates/1913.
(14) Gambardella, P.; et al. *Nat. Mater.* **2009**, *8*, 189–193. Barth, J. V. *Surf. Sci.* **2009**, *603*, 1533–1541.
(15) Meunier, B. *Chem. Rev* **1992**, *92*, 1411–1456. Purrello, R.; Gurrieri, S.; Lauceri, R. *Coord. Chem. Rev.* **1999**, *190−192*, 683–706. Beletskaya, I.; Tyurin, V. S.; Tsivadze, A. Y.; Guilard, R.; Stern, C. *Chem. Rev.* **2009**, *109*, 1659–1713. Forrest, S. R. *Chem. Rev.* **1997**, *97*, 1793–1896.
(16) Shi, Z.; Lin, N. *J. Am. Chem. Soc.* **2009**, *131*, 5376–5377.
(17) Barlow, S. M.; Raval, R. *Surf. Sci. Rep* **2003**, *50*, 201–341. Ernst, K. H. *Top. Curr. Chem.* **2006**, *265*, 209–252.
(18) Yokoyama, T.; Kamikado, T.; Yokoyama, S.; Mashiko, S. *J. Chem. Phys.* **2004**, *121*, 11993–11997.
(19) Weigelt, S.; Busse, C.; Petersen, L.; Rauls, E.; Hammer, B.; Gothelf, K. V.; Besenbacher, F.; Linderoth, T. R. *Nat. Mater.* **2006**, *5*, 112–117. Bombis, C.; Weigelt, S.; Knudsen, M. M.; Norgaard, M.; Busse, C.; Laegsgaard, E.; Besenbacher, F.; Gothelf, K. V.; Linderoth, T. R. *ACS Nano* **2009**, *4*, 297–311.
(20) Bombis, C.; Ample, F.; Lafferentz, L.; Yu, H.; Hecht, S.; Joachim, C.; Grill, L. *Angew. Chem., Int. Ed.* **2009**, *48*, 9966–9970.
(21) Heim, D.; Seufert, K.; Auwärter, W.; Aurisicchio, C.; Fabbro, C.; Bonifazi, D.; Barth, J. V. *Nano Lett.* **2009**, *10*, 122–128.
(22) Jung, T.; Schlittler, R.; Gimzewski, J. *Nature* **1997**, *386*, 696–698.
(23) Yokoyama, T.; Yokoyama, S.; Kamidado, T.; Mashiko, S. *J. Chem. Phys.* **2001**, *115*, 3814. Ecija, D.; Trelka, M.; Urban, C.; Mendoza, P. d.; Mateo-Martín, E.; Rogero, C.; Martín-Gago, J. A.; Echavarren, A. M.; Otero, R.; Gallego, J. M.; Miranda, R. *J. Phys. Chem. C* **2008**, *112*, 8988–8994.
(24) Moresco, F.; Meyer, G.; Rieder, K.-H.; Ping, J.; Tang, H.; Joachim, C. *Surf. Sci.* **2002**, *499*, 94–102. Auwarter, W.; Weber-Bargioni, A.; Riemann, A.; Schiffrin, A.; Groning, O.; Fasel, R.; Barth, J. V. *J. Chem. Phys.* **2006**, *124*, 194708–6. Zotti, L. A.; Teobaldi, G.; Hofer, W. A.; Auwärter, W.; Weber-Bargioni, A.; Barth, J. V. *Surf. Sci.* **2007**, *601*, 2409–2414. Weber-Bargioni, A.; Auwärter, W.; Klappenberger, F.; Reichert, J.; Lefrançois, S.; Strunskus, T.; Wöll, C.; Schiffrin, A.; Pennec, Y.; Barth, J. V. *ChemPhysChem* **2008**, *9*, 89–94.
(25) Fleischer, E. B.; Stone, A. L. *Chem. Commun.* **1967**, 332.
(26) Auwärter, W.; Klappenberger, F.; Weber-Bargioni, A.; Schiffrin, A.; Strunskus, T.; Wöll, C.; Pennec, Y.; Riemann, A.; Barth, J. V. *J. Am. Chem. Soc.* **2007**, *129*, 11279–11285.

Chart 1. Porphyrin Derivative **1** Used as a Building Block for the Coordination Polymers[a]

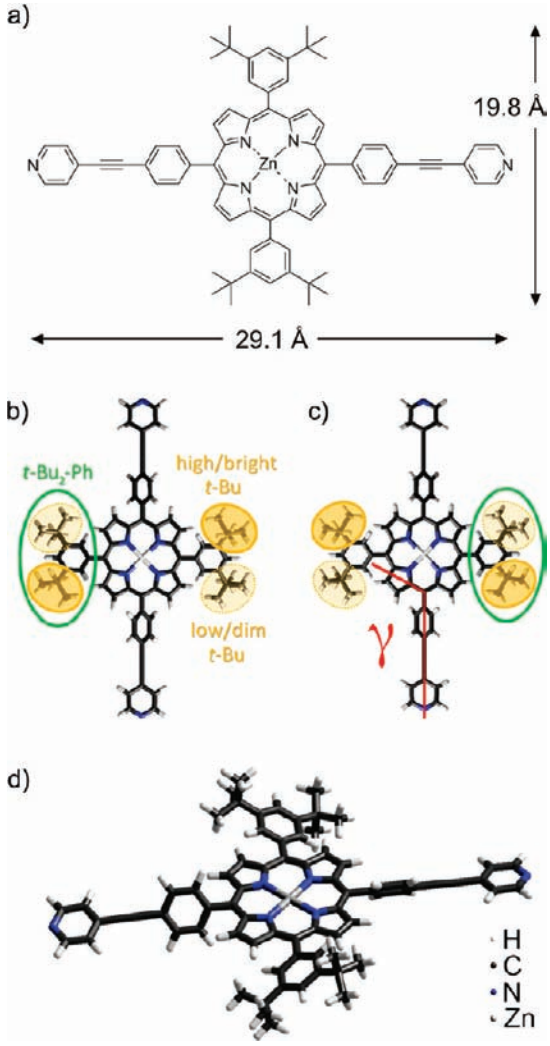

[a] (a) Molecular dimensions are extracted from PM3 calculations performed using the HyperChem molecular modeling package.[28] (b, c) Schematic illustration of adsorption-induced molecular deformations resulting in conformational surface enantiomers β (b) and α (c). Rotation of the *t*-Bu_2Ph group results in one *t*-Bu constituent being higher than its counterpart; angle γ of the PhC≡CPyr leg can deviate from the intrinsic value of 118°. (d) 3D view showing the converse rotation of opposite *t*-Bu_2Ph substituents.

are well documented in literature.[18,22] The lower *t*-Bu from each *meso*-position are going to act as legs, interacting through van der Waals forces with the metallic substrate and decoupling the core of the porphyrin macrocycle from the substrate (cf. Chart 1d). In addition, MM+ molecular mechanics simulations show that the PhC≡CPyr legs are quite flexible (cf. Supporting Information, Figure S1). The angle γ between the *meso* PhC≡CPyr leg and the porphyrin core can vary from the equilibrium position up to 15° degrees toward the *t*-Bu_2Ph substituents with an energy cost of less than 20 kcal/mol. Due to the conformational properties, i.e., the flexibility of the PhC≡CPyr substituents and the rotability of all *meso*-substituents, *t*-Bu_2Ph groups included, tetrapyrrolic module **1** deconvolutes into two stereoisomers upon surface confinement,[18] which play a major role in the structure of the polymer chains. Note that as a consequence of the *t*-Bu rotations there is a collective macrocycle distortion similar to that reported before for a related compound,[27] which consists in two downward and two upward twisted pyrroles. Very remarkably, the overall intramolecular and molecule−substrate interactions favor the exclusive existence of two conformers, in which the dihedral angle of opposing substituents is converse. The possible conformers, where the dihedral angle of opposing substituents is the same, are not detected.

Figure 1a shows a large-scale STM image of the Cu(111) surface after the deposition of 0.2 ML of module **1** at a substrate temperature of 350 K. The surface steps appear completely covered with molecules. Images taken at lower coverage (not shown) indicate that the porphyrins decorate completely the steps before spontaneous ordering takes place on the terraces, indicating a high mobility at 350 K. At higher coverage, porphyrin derivative **1** self-assembles into one-dimensional chains of variable length and an apparent width of 19.5 Å, which fits well to the lateral dimension of a single molecule flatly adsorbed on the surface (cf. Chart 1a). Regarding the orientation, all chains present a striking flexibility as we can distinguish linear and curved segments. The autocorrelation plot, a mathematical tool to detect periodic patterns (Figure 1a, cf. Supporting Information), clearly reveals periodic features with a intermolecular center-to-center spacing of roughly 32 Å and shows that chains are aligned within an ±15° corridor with respect to the dense-packed directions of the Cu(111) surface atomic lattice (see below). In addition, most of the chains do not interconnect to each other, even at higher coverage (Figure 1b), which testifies the presence of repulsive forces between the chains, similarly encountered for H-bonded 1D surface-confined polymers.[29]

Taking a closer look at the assemblies, we can resolve individual molecules (Figure 2a). The distance between the centers of two adjacent molecules is 32.7 Å, in agreement with the autocorrelation plot displayed in Figure 1a. Based on the molecular dimensions, this spacing indicates a distance of 3.6 Å between two N atoms of subsequent pyridyl groups, large enough for accommodating a metal−organic bonding interaction, such as a two-fold pyridyl−Cu−pyridyl coordination, with a projected Cu−N distance of 1.8 Å (Figure 2b−d). At 350 K, Cu(111) provides sufficient Cu adatoms on the surface to interact with the pyridyl groups[30] thus promoting the Cu-mediated head-on coupling of two pyridyl functions.[31−33] However, Cu centers are not resolved in our STM images, in agreement with former reports,[8,10,11,34,35] presumably due to an electronic effect.[7]

(27) Fendt, L.; Stöhr, M.; Wintjes, N.; Enache, M.; Jung, T. A.; Diederich, F. *Chem.—Eur. J.* **2009**, *15*, 11139–11150.
(28) *Hyperchem*, version 7.5; HyperCube, Inc.: Gainesville, Florida, 2003.
(29) Barth, J. V.; Weckesser, J.; Cai, C.; Günter, P.; Bürgi, L.; Jeandupeux, O.; Kern, K. *Angew. Chem. Int. Ed* **2000**, *39*, 1230–1234. Schiffrin, A.; Riemann, A.; Auwärter, W.; Pennec, Y.; Weber-Bargioni, A.; Cvetko, D.; Cossaro, A.; Morgante, A.; Barth, J. V. *Proc. Natl. Acad. Sci. U.S.A.* **2007**, *104*, 5279–5284.
(30) Karimi, M.; Tomkowski, T.; Vidali, G.; Biham, O. *Phys. Rev. B* **1995**, *52*, 5364. Perry, C. C.; Haq, S.; Frederick, B. G.; Richardson, N. V. *Surf. Sci.* **1998**, *409*, 512.
(31) Eichberger, M.; Marschall, M.; Reichert, J.; Weber-Bargioni, A.; Auwärter, W.; Wang, R. L. C.; Kreuzer, H. J.; Pennec, Y.; Schiffrin, A.; Barth, J. V. *Nano Lett.* **2008**, *8*, 4608.
(32) Klappenberger, F.; Weber-Bargioni, A.; Auwärter, W.; Marschall, M.; Schiffrin, A.; Barth, J. V. *J. Chem. Phys.* **2008**, *129*, 214702.
(33) Shi, Z.; Lin, N. *ChemPhysChem* **2010**, *11*, 97–100.
(34) Clair, S.; Pons, S.; Fabris, S.; Baroni, S.; Brune, H.; Kern, K.; Barth, J. V. *J. Phys. Chem. B* **2006**, *110*, 5627.
(35) Classen, T.; Lingenfelder, M.; Wang, Y.; Chopra, R.; Virojanadara, C.; Starke, U.; Costantini, G.; Fratesi, G.; Fabris, S.; de Gironcoli, S.; Baroni, S.; Haq, S.; Raval, R.; Kern, K. *J. Phys. Chem. A* **2007**, *111*, 12589.

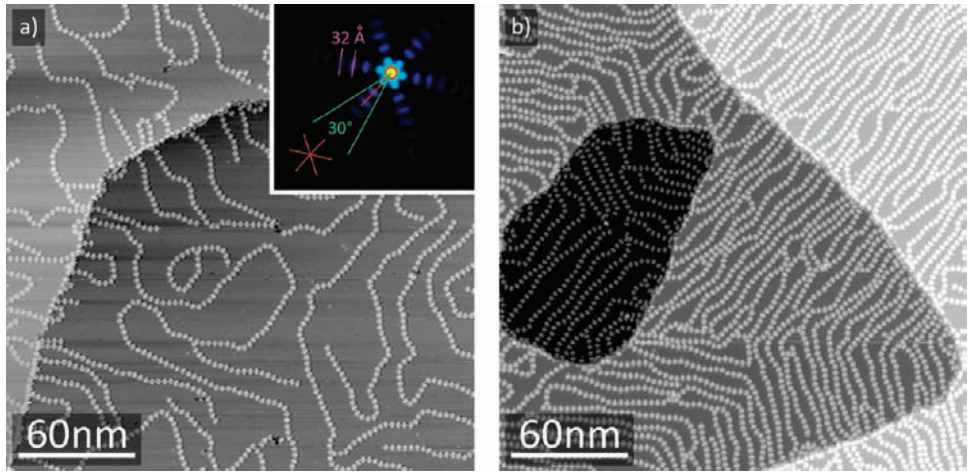

Figure 1. STM images of a Cu(111) surface taken at 6 K after the evaporation of (a) 0.2 ML ($V = 1.0$ V, $I = 0.25$ nA) and (b) 0.4 ML ($V = -1.0$ V, $I = 0.1$ nA) of porphyrin **1** at a substrate temperature of about 350 K. Inset in (a): autocorrelation plot of image, where the dense-packed directions of the Cu(111) surface are depicted in red.

Recently, we have reported an identical coupling motif after the deposition of a cis-like isomer of module **1** on Cu(111) surfaces, which resulted, triggered by the different molecular symmetry, in the formation of macrocyclic supramolecules.[21] Although the projected Cu−N distance is 1.8 Å, different phenomena such as the bending of PhC≡CPyr binding linkers and the possible lifting of the metal center,[36] considering that Cu−pyridyl interaction is directional, could vary this distance.[21] In full agreement with our results, nonflexible straight metal−organic chains have been reported on Cu(100) based on a two-fold coordination geometry between pyridyl functions and Cu metal centers,[8] with a Cu−N distance of 1.9 Å (theoretical DFT simulations performed for an isolated pyridyl−Cu−pyridyl complex gave a value of 1.8 Å).[31] Alternatively, a 3D polymeric network comprised of 2D $Cu(HCO_2)_2$ layers fused together by linear pyrazine spacers (forming Cu−pyrazine−Cu chains) was reported to show Cu−N distance of 2.0 Å as determined by a X-ray diffraction analysis.[37]

In bulk coordination chemistry (i.e., at the solid state or in solution), Cu(I) and Cu(II) metal ions typically coordinate to pyridyl ligands with a four-fold symmetry;[38] while the confinement of molecular tectons to a surface induce unusual two-fold coordination motifs,[8,10,11,32,35] such as the pyridyl−Cu−pyridyl interaction motif described here. The steric restriction among the molecular building blocks and the charge equilibration provided by the metal surface can favor reduced metal−ligand coordination ratios.[10] Although generally there is a repulsive interaction among chains, they are sometimes interlocked. Hereby we distinguish two different coupling schemes between chains (cf. Supporting Information, Figure S2): (i) van der Waals interactions between the pyridyl functions of one chain and the *t*-Bu_2Ph of another one and (ii) frequent three-fold Cu-mediated coordination motifs that give rise to nodal arrangements. From a statistical comparison between the Cu-coordinated motifs (Figure 1) we can conclude that the two-fold motif is predominant. The abundance of the two-fold Cu-based coordination (and thus the existence of linear assemblies as compared to bidimensional networks based on trifurcated coordination nodes) is tentatively explained by a considerable steric hindrance between the three molecules in the node (cf. Supporting Information, Figure S2).

Recently, the formation of chainlike structures for similar *trans*-bis(4-cyanophenyl)-substituted molecules has been reported,[27,39] where the main difference with compound **1** is the use of the cyanophenyl ligands instead of the pyridyl moieties present in our molecular module. The binding motif is suggested to be based on dipolar CN···CN interactions together with CN···H−C hydrogen bonds. Judging from the published data, these weaker interactions result in the formation of less linear chains that are more frequently ramified by a trimeric motif as compared to the coordination polymer reported here. An early study by Yokoyama et al.[40] already explored such CN···CN interactions to form sequential porphyrin aggregates. Hereby, the elbows of the herringbone reconstruction of the Au(111) surface proved crucial to stabilize the chainlike assemblies. As a consequence of the antiparallel coupling of the cyano groups, including a lateral offset and the reduced length of their module, the intermolecular distances are considerably shorter than in our coordination polymers. The metal−ligand coupling motif reported here (vide infra) results in an average chain length clearly exceeding the reported values,[40] independent of the substrate.

Figure 3 summarizes the assembling modes giving rise to the different polymeric structures and their arrangements on the surface (straight and zig−zag lines, turns, and U-turns). As a result of the rotation of the *t*-Bu_2Ph substituents and the flexibility of the PhC≡CPyr binding functions, the porphyrin molecule presents two configurational enantiomers upon adsorption. These enantiomers, labeled as α and β, are depicted in panels e−f of Figure 3. Statistical treatment shows that the α:β ratio on the surface is 1:1. Both enantiomers are locked to the substrate by an alignment of the double-lobed features (i.e., the *t*-Bu_2Ph) with the dense-packed directions of the Cu(111) surface. Then, since Cu(111) is a fcc crystal, there are three

(36) Seitsonen, A. P.; Lingenfelder, M.; Spillmann, H.; Dmitriev, A.; Stepanow, S.; Lin, N.; Kern, K.; Barth, J. V. *J. Am. Chem. Soc.* **2006**, *126*, 5634–5635.
(37) Manson, J. L.; Lecher, J. G.; Gu, J.; Giser, U.; Schlueter, J. A.; Henning, R.; Wang, X.; Schultz, A. J.; Koo, H.-J.; Whangbo, M.-H. *Dalton Trans.* **2003**, 2905–2911.
(38) Osako, T.; Tachi, Y.; Taki, M.; Fukuzumi, S.; Itoh, S. *Inorg. Chem.* **2001**, *40*, 6604. Dietrich-Buchecker, C. O.; Guilhem, J.; Pascard, C.; Sauvage, J. P. *Angew. Chem., Int. Ed.* **1990**, *29*, 1154.
(39) Wintjes, N.; Hornung, J.; Lobo-Checa, J.; Voigt, T.; Samuely, T.; Thilgen, C.; Stöhr, M.; Diederich, F.; Jung, T. A. *Chem.−Eur. J.* **2008**, *14*, 5794–5802.
(40) Yokoyama, T.; Yokoyama, S.; Kamikado, T.; Okuno, Y.; Mashiko, S. *Nature* **2001**, *413*, 619–621.

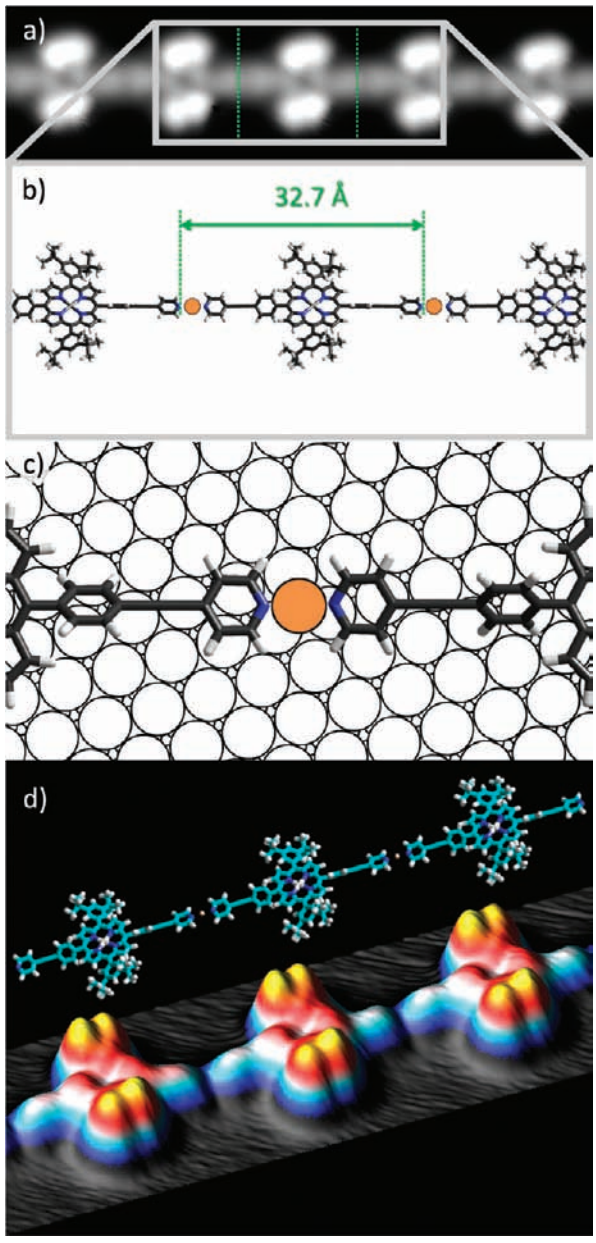

Figure 2. (a) High-resolution STM image of a straight coordination chain segment of porphyrin derivative **1** on Cu(111) ($V = -1.0$ V, $I = 77$ pA). (b) Schematic plot of the pyridyl−Cu−pyridyl linear chaining arrangement (3D view). (c) Top-view model for the pyridyl−Cu−pyridyl coupling motif. (d) Three-dimensional view and Hyperchem model of (a), displaying a string consisting only of one surface enantiomer.

possible orientations of each enantiomer on the surface. In each *t*-Bu_2Ph substituent, one *t*-Bu group appears brighter than the other. The PhC≡CPyr functions form an angle of −15° or +15° (enantiomer α and β, respectively) with respect to the dense-packed directions of the substrate and, consequently, with respect to the double-lobed features corresponding to the *t*-Bu_2Ph substituents. The likely origin of this nonparallel alignment of the PhC≡CPyr functions and the double-lobed *t*-Bu_2Ph features are detailed in the Supporting Information (Figure S1). As a result of the existence of two enantiomers and three equivalent orientations per enantiomer, there exists a set of different chain−connector motifs (cf. Supporting Information, Figure S3), the sequence of which decides chain morphology, allowing even the existence of 1D supramolecular isomeric segments.

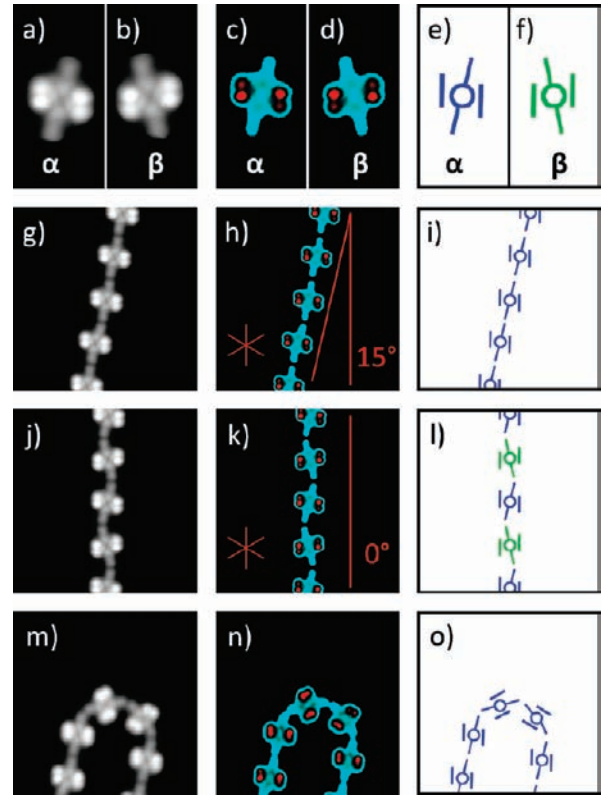

Figure 3. (a, b) STM images of the two conformational isomers α and β of porphyrin derivative **1** on Cu(111). (c, d) Images (a and b) reproduced in enhanced contrast to visualize the different apparent heights of the *t*-Bu groups (cf. Chart 1b,c). The vertical line represents a dense-packed substrate direction and thus a projection of the mirror plane. (e, f) Schematic representation of both isomers. (g−i) Portion of straight chain constituted only by α enantiomers. The chain direction includes an angle of 15° with a dense-packed Cu(111) direction (red vertical line, the red star indicates all dense-packed directions. (j−l) Zig−zag chains constituted by alternating enantiomers; the overall segment orientation is aligned with a dense-packed Cu(111) direction. (m−o) Example of a U-turn. Tunneling parameters: (a−d), (g), (h), (j), (k): $V = 1.0$ V, $I = 0.2$ nA; (m and n): $V = 0.94$ V, $I = 0.36$ nA.

By a detailed analysis, checking the orientation of the PhC≡CPyr functions and the different apparent heights of the *t*-Bu_2Ph decorations, we observe that straight chains are formed by the same enantiomer (α or β, Figure 3, panels g−i) while zig−zag chains are constituted by an alternate sequence of α and β enantiomers (Figure 3, panels j−l).

In nice agreement with the corridor of the autocorrelation plot depicted in Figure 1a, the mean orientation of the straight chains is either −15° (consisting of enantiomers α, chain segment in Figure 3, panels g and h) or +15° (consisting of enantiomers β, not shown here) with respect to the close-packed directions of the Cu(111) surface; whereas the zig−zag segments are just parallel to them. Representing the extreme case for curved chain segments, U-turns seem to be constituted by the same enantiomer (α or β), but with adjacent linker units 'locked-in' to a different (and consecutive) dense-packed direction of the substrate. Panels m−o of Figure 3 nicely show the molecular structure of a U-turn: starting from left to right, the first molecule is 'locked-in' a high-symmetry direction followed by three molecules that are each rotated by 60° with respect to their respective consecutive neighbors. The fourth molecule in the chain ends up having an orientation the same as that of the first one, thus completing the U-turn. In addition, U-turns formed by three molecules were also very rarely observed. In this

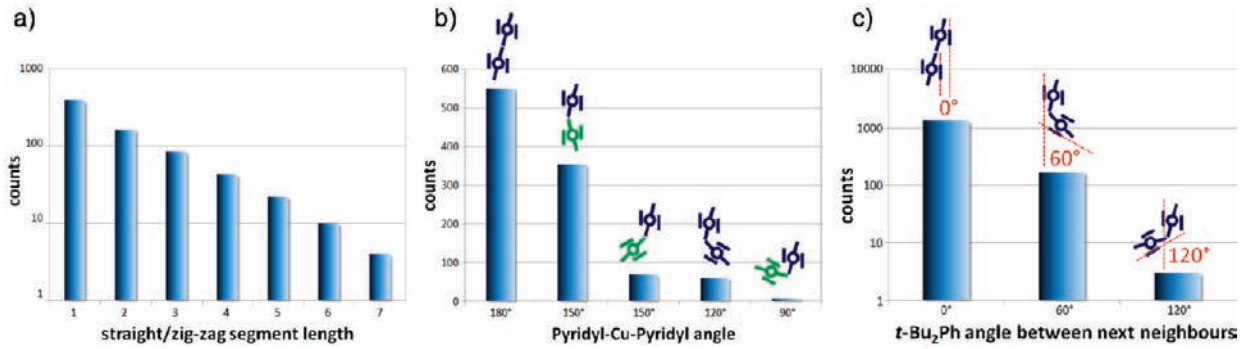

Figure 4. Statistical analysis of coordination polymers on Cu(111). (a) The number of molecules in a straight/zig−zag chain segment: The occurrence of straight/zig−zag chains segments decreases exponentially with increasing length, highlighting the statistical assembly process and excluding effects stabilizing a preferred straight/zig−zag segment length. (b) Angle formed by the PhC≡CPyr legs in the PhC≡CPyr−Cu−PyrC≡CPh coordination motif. (c) Angles of *t*-Bu substituents between two successive neighbors (compare models). The probability of finding two neighboring molecules in the same orientation is about an order of magnitude higher than a directional change of 60°. Directional changes by 120° between adjacent modules are extremely rare.

particular structural mode the necessary 120° angle is provided by a more pronounced bending of the PhC≡CPyr functions.

From a statistical analysis of the length of the straight/zig−zag segments and the curvature of the chains, we observed that the length of the chains displays an exponential decay, reflecting that shorter, straight or zig−zag segments are more likely (Figure 4a). This observation excludes that specific segment lengths are favored, for example due to stabilizing effects invoked by the commensurability with the surface atomic lattice. In addition, adjacent porphyrin molecules exhibiting the same orientation (i.e., 0° rotation) are far more common than those with a rotation of 60° or even 120° (Figure 4b and c). This fact does not depend on the enantiomeric character of the molecules involved, which justifies why the amounts of straight (same enantiomers) or zig−zag (alternating enantiomers) segments are similar. These results are consistent with the autocorrelation plot in Figure 1a, where the intensity of the periodic features presents an exponential decay. As a consequence of these statistics, there is a preference for the formation of a straight or a 30° deviated PhC≡CPyr−Cu−PyrC≡CPh coordination−bonding interaction. This is associated with metal−ligand interactions the directional nature of which results in a higher bonding energy for the straight (or 30° deviated) than for the more curved PhC≡CPyr−Cu−PyrC≡CPh coordination motifs.

It is interesting to compare these results with the folding of covalent polymers adsorbed on surfaces. Thereby,[41] the frequency and combination of each of the coupling motifs results in an overall aspect of the polymer chains in which straight/zig−zag segments combine with the 60°/120° coupling motifs to give rise to a versatile folding of the polymers up to 180°.

To further probe the nature of the metal-based coordination coupling between the porphyrin monomers and to study induced polymer folding, we performed control experiments on Ag(111) surfaces. When porphyrin module **1** is deposited on Ag(111) held at 390 K, it self-assembles into a hexagonal porous network that will be discussed in detail elsewhere. Following codeposition of Cu adatoms at 390 K, the supramolecular pattern undergoes a dramatic structural change. Now, the surface is covered by chains with the same appearance as those observed on Cu(111) (Figure 5), which, by analogy, are recognized as Cu-coordinated porphyrin polymers. Thus, the pyridyl−Cu−pyridyl coordination scheme overrides a considerable lattice constant difference between both surfaces ($d_{Cu(111)} = 2.56$ Å and $d_{Ag(111)} = 2.88$ Å), suggesting a robust coupling motif. While the overall topographic appearance of these coordination polymers is strikingly similar on both surfaces, three structural differences are observed at the molecular level: (i) the projected Cu−N distance is only 1.4 Å on Ag(111) versus the 1.8 Å value on Cu(111) (this discrepancy could be related to a larger adsorption height or different surface conformational adaptation (inner core, flexible PhC≡Cpyr legs) of the molecule on Ag(111) compared to Cu(111), as the former is a relatively inert substrate); (ii) on Ag(111) the porphyrin molecules are also frequently rotated 30° with respect to close-packed lattice directions, while on Cu(111) only three orientations (i.e., 60° rotations) of the modules were detected, indicating again a reduced molecule−substrate interaction on Ag surfaces; (iii) trifurcated joints are more common on Ag(111) than on Cu(111) surfaces as a consequence of different mobilities of the porphyrin and Cu-adatoms on both surfaces together with a varied adatom density. Regardless these minor structural dissimilarities, the results confirm our conclusion that the supramolecular multi-porphyrin polymers obtained by the deposition of **1** on Cu (111) or by the mixing of **1** with Cu adatoms on Ag(111) are coupled through pyridyl−Cu−pyridyl coordination−bonding interactions.

In order to test the strength of the metal−ligand interactions and to directly probe the flexibility of the coordination polymer, molecular manipulation experiments were carried out. To this end, we employed the STM tip as a tool to bend segments of the multi-porphyrin chain on both Cu(111) and Ag(111) surfaces (Figure 6). Starting from regular imaging conditions (typical tunneling resistance $R \approx 10$ GΩ) in which the chains are unaffected by the STM tip (panels a and d of Figure 6), the tip is brought closer to the surface to increase the interaction with the adsorbates ($R \approx 20$ MΩ), and laterally translated across a terminal porphyrin (the tip path is indicated by the white arrows in panels c and f of Figure 6). After the first manipulation step, the surface is imaged again to detect the changes in the chain orientation (panels b and e of Figure 6). Applying this manipulation procedure, we were able not only to move the terminating unit of the multi-porphyrin chains but also to displace entire segments without breaking the 1D assemblies. For example, Figure 6f highlights the shifting of an assembly termination involving three porphyrin units within a single

(41) Mena-Osteritz, E.; Meyer, A.; Langeveld-Voss, B. M. W.; Janssen, R. A. J.; Meijer, E. W.; Bäuerle, P. *Angew. Chem., Int. Ed* **2000**, *39*, 2679–2684. Lei, S.-B.; Wan, L.-J.; Wang, C.; Bai, C.-L. *Adv. Mater.* **2004**, *2004*, 828–831. Lei, S.-B.; Deng, K.; Yang, Y.-L.; Zeng, Q.-D.; Wang, C.; Ma, Z.; Wang, P.; Zhou, Y.; Fan, Q.-L.; Huang, W. *Macromolecules* **2007**, *40*, 4552–4560.

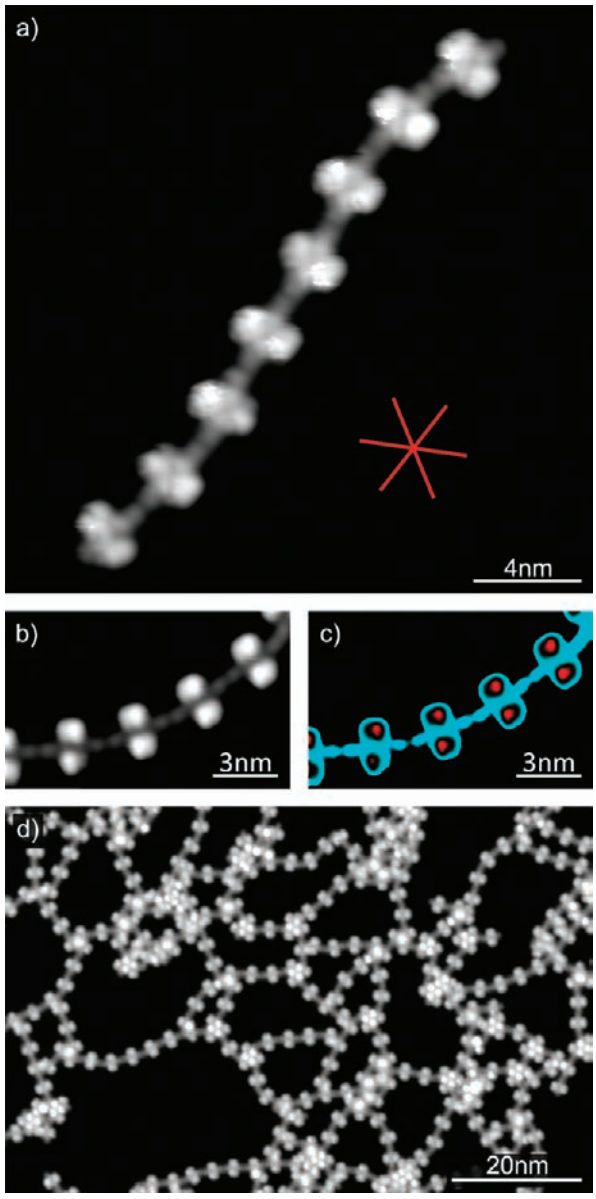

Figure 5. (a) Molecular chain segment of module **1** on Ag(111), fabricated by codeposition of molecular modules and Cu adatoms ($V = -1.0$ V, $I =$ 77 pA). The red star indicates the close-packed directions. (b) High-resolution image of a chain segment with adapted contrast (c) to highlight the molecular conformation (compare Figure 3h and k). (d) STM image of a Ag(111) surface after the deposition of 0.2 ML of module **1** and subsequent evaporation of copper ($V = 1$ V, $I = 0.2$ nA).

manipulation process. Remarkably, on Ag(111) surfaces the chain segments could also be reversibly brought back to their initial position. These results highlight the flexibility of such coordination polymers and the considerable intrapolymer cohesion, given by the strength of the Cu−N bond, which overrides the substrate bonding at specific sites.

Regarding stability, metal−organic coordinated networks on surfaces can be classified midway between the weak noncovalent interactions such as van der Waals, $\pi-\pi$, dipole−dipole, and H-bonding[42] and the robust covalent polymers.[12,43,44] However,

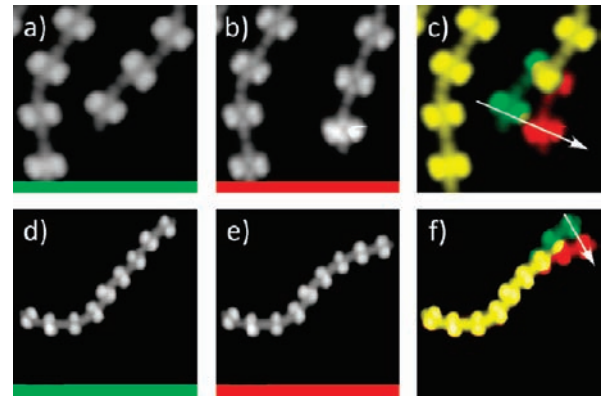

Figure 6. Molecular manipulation of the Cu-mediated coordination multiporphyrin polymers on Cu(111) (a−c) and on Ag(111) (d−f) surfaces. Tunneling parameters: (a and b) $V = 1.0$ V, $I = 0.25$ nA. (c) Manipulation parameters: $V = -0.05$ V, $I = 8.0$ nA. (d and e) $V = -1.0$ V, $I = 0.1$ nA. (f) Manipulation parameters: $V = -0.2$ V, $I = 10.0$ nA.

one main feature and great advantage of metal−organic networks is that the strength and lability of the coordination bonds are such that adaptive materials can be readily prepared because of the reversibility of these interactions. In contrast, once made, covalent polymers contain defects that are "locked in", resulting in nanostructured materials with low periodic ordering and little adaptivity,[12,43] as testified by the limited quality of arrays reported on surfaces.[44]

Conclusions

In summary, we have described the metal-directed assembly of coordination polymers on Cu(111) and Ag(111) surfaces by using a *de novo* porphyrin derivative and Cu adatoms as tectons exploiting two-fold pyridyl−Cu−pyridyl coupling motifs. These polymers display a striking flexibility in their morphology, which is based on the two enantiomeric conformations of the molecule on the surface. Together with site-specific surface anchoring, this gives rise to straight and zig−zag segments, turns, and U-turns, the sequence and arrangement of which result in the overall structure of the chains. Notably, we observe the formation of isomeric supramolecular segments in the chains. Statistical analysis reflects the directionality of the metal−ligand bonds, showing the majoritary formation of perfectly straight or slightly bent pyridyl−Cu−pyridyl coupling motifs.

Remarkably, we have been able to reversibly move the tails of the chains, involving more than two molecules. As a consequence, the formed coordination polymers are expected to be useful for connecting other nanoscale objects[45] or even to transport charges. Furthermore, porphyrin derivatives can be modified (e.g., by altering their metallic center or selective axial ligation) to act as platforms for further construction of highly functional monodimensional nanostructures by coordination of

(42) Barth, J. V. *Annu. Rev. Phys. Chem.* **2007**, *58*, 375–407. Elemans, J. A. A. W.; Lei, S.; Feyter, S. D. *Angew. Chem., Int. Ed.* **2009**, *48*, 7298–7333. Bonifazi, D.; Mohnani, S.; L-Pallas, A. *Chem.—Eur. J.* **2009**, *15*, 7004–7025.

(43) Grill, L.; Dyer, M.; Lafferentz, L.; Persson, M.; Peters, M. V.; Hecht, S. *Nat. Nanotechnol.* **2007**, *2*, 687. Veld, M.; Iavicoli, P.; Haq, S.; Amabilino, D. B.; Raval, R. *Chem. Commun.* **2008**, 1536. Treier, M.; Fasel, R.; Champness, N. R.; Argent, S.; Richardson, N. V. *Phys. Chem. Chem. Phys.* **2009**, *11*, 1209.

(44) Weigelt, S.; Busse, C.; Bombis, C.; Knudsen, M. M.; Gothelf, K. V.; Strunskus, T.; Wöll, C.; Dahlbom, M.; Hammer, B.; Laegsgaard, E.; Besenbacher, F.; Linderoth, T. R. *Angew. Chem., Int. Ed* **2007**, *119*, 9387. Zwaneveld, N. A. A.; Pawlak, R.; Abel, M.; Catalin, D.; Gigmes, D.; Bertin, D.; Porte, L. *J. Am. Chem. Soc.* **2008**, *130*, 6678–6679. Lipton-Duffin, J. A.; Ivasenko, O.; Perepichka, D. F.; Rosei, F. *Small* **2009**, *5*, 592.

(45) Clair, S.; Pons, S.; Brune, H.; Kern, K.; Barth, J. V. *Angew. Chem., Int. Ed.* **2005**, *44*, 7294–7297.

electronically, optically, or magnetically active ligands. The extension of our strategy at insulating substrates seems feasible and could pave the way for the design of adaptive molecular wires based on flexible modules.

Experimental Section

All STM experiments were performed in a custom-designed ultrahigh vacuum (UHV) system providing a base pressure below 1×10^{-10} mbar.[46] The monocrystalline Cu(111) and Ag(111) substrates were cleaned by repeated Ar^+ sputtering cycles at an energy of 800 eV, followed by annealing at 730 K for 10 min. Subsequently, a submonolayer coverage of porphyrin derivative **1** was deposited by organic molecular beam epitaxy from a thoroughly degassed quartz crucible held at 680 K. During deposition, the Cu(111) or the Ag(111) surfaces were kept at 340 or 373 K, respectively, and the pressure remained $<5 \times 10^{-10}$ mbar. Cu atoms were evaporated from a homemade water-cooled cell by resistively heating a W filament surrounded by a Cu wire of high purity (99.9999%). All STM images were acquired by employing a low-temperature CreaTec-STM[47] with the sample held at 6 K using electrochemically etched W tips. In the figure captions, *V* refers to the bias voltage applied to the sample. Regarding coverage, we define 1 ML as one surface fully covered by molecules. Simulations were performed in the framework of the Hyperchem 7.5 Software Package.[28] The WSxM software was used for the analysis of STM images.[48]

Acknowledgment. Work supported by the ESF project Fun-Smarts and the Munich Center for Advanced Photonics (MAP). D.B. especially acknowledges the University of Namur, the Belgian National Research Foundation (FRS-FNRS, through the Contracts 2.4.625.08 F and F.4.505.10.F), the "Loterie Nationale", and the Région Wallonne through the "SOLWATT" program (Contract 850551), the 'TINTIN' ARC project from the Belgian French Community (Contract 09/14-023). D.E. thanks the European Commission for support through the Marie Curie IntraEuropean Fellowship for Career Development FP7 program (project Nanolanta, Proposal 235722).

Supporting Information Available: Discussion about the topographic appearance and conformation of porphyrin 1 on Cu(111). Graph of the energy cost versus the angle of the bending of one PhC≡CPyr leg toward the core of the porphyrin of an isolated molecule. Scheme and total charge density plot of the converse rotation of the two *t*-Bu moieties within the *t*-Bu_2Ph group. Brief explanation of the autocorrelation plot technique. STM images of the 3-fold trimeric motifs and the pyridyl-*t*-Bu noncovalent bond. Schemes of the coupling motifs of the porphyrin on Cu(111). Complete ref 14. This material is available free of charge via the Internet at http://pubs.acs.org.

JA1010527

(46) Auwärter, W.; Schiffrin, A.; Weber-Bargioni, A.; Pennec, Y.; Riemman, A.; Barth, J. V. *Int. J. Nanotechnol* **2008**, *5*, 1171.
(47) *CreaTec-STM*; CreaTec: Erligheim, Germany.
(48) Horcas, I.; Fernández, R.; Rodríguez, J. M.; Colchero, J.; Gómez-Herrero, J.; Baró, A. M. *Rev. Sci. Instrum.* **2007**, *78*, 013705.